THE ASTROPHYSICAL JOURNAL, 439:191–201, 1995 January 20

CCD PHOTOMETRY OF GLOBULAR CLUSTER CORE STRUCTURE. II. *U*-BAND PROFILES FOR 15 CANDIDATE COLLAPSED-CORE CLUSTERS

PHYLLIS M. LUGGER[1,2] AND HALDAN N. COHN[1,2]
Department of Astronomy, Indiana University, Swain West 319, Bloomington, IN 47405;
E-mail: lugger@astro.indiana.edu, cohn@astro.indiana.edu

AND

JONATHAN E. GRINDLAY[1]
Department of Astronomy, Harvard University, Center for Astrophysics, 60 Garden Street, Cambridge, MA 02138;
E-mail: josh@cfa255.harvard.edu
Received 1994 June 16; accepted 1994 July 27

ABSTRACT

We present *U*-band CCD surface brightness profiles for 15 of the 21 globular clusters that have been identified as having collapsed cores by Djorgovski & King (1986). Fourteen of the clusters were observed with the Cerro Tololo 4 m telescope; NGC 7078 was observed with the Canada-France-Hawaii 3.6 m telescope. We have fitted the profiles with seeing-convolved power laws, both with and without cores, to assess the evidence for central power-law structure and to place upper limits on core radius r_c. We find nine of the clusters (NGC 5946, NGC 6284, NGC 6293, NGC 6325, NGC 6342, NGC 6558, NGC 6624, NGC 6681, and NGC 7078) to have unresolved cores, with upper limits $r_c \leq 1''.9$. Three of the clusters (NGC 6453, NGC 6522, and NGC 7099) have marginally resolved cores, with upper limits in the range $2''.7 \leq r_c \leq 3''.4$. The remaining three clusters (NGC 6355, NGC 6397, and NGC 6752) have resolved cores. Of the latter three clusters, NGC 6355 and NGC 6752 are consistent with single-mass King model structure. The median cluster distances are 9.2 kpc for those with unresolved cores, 7.2 kpc for those with marginally resolved cores, and 4.1 kpc for those with resolved cores.

The 13 clusters that do not resemble single-mass King models have central power-law structure with surface brightness slopes in the range of $d \ln S/d \ln r = -0.6$ to -0.8. These slopes are consistent with the models of Grabhorn et al. (1992) for clusters evolving beyond core collapse. The models include a centrally concentrated population of nonluminous remnants with masses in the range 1.2–1.4 $M_\odot$, thus providing evidence for significant neutron star populations in most of our cluster sample. This finding is consistent with the observation of centrally concentrated low-mass X-ray binary and millisecond pulsar populations in several clusters.

Subject headings: celestial mechanics, stellar dynamics — globular clusters: general — techniques: photometric

1. INTRODUCTION

It has been known since the mid-1970s that some globular clusters have extremely compact cores that appear unresolved by digital ground-based imaging (Newell & O'Neil 1978). The observed central surface brightness profiles of these clusters, such as M15 (= NGC 7078), are characterized by power-law cusps down to the seeing limit, rather than resembling single-mass King models with resolved cores (Djorgovski & King 1984; Lugger et al. 1987, hereafter Paper I). The theory of globular cluster dynamical evolution predicts the development of such power-law structure during core collapse (see, e.g., Cohn 1980). Djorgovski & King (1984) have thus classified clusters with a central surface brightness cusp as "post–core collapse" (PCC).[3]

Djorgovski & King (1986) identified 21 clusters as being PCC, in a large-scale survey of core structure of 123 clusters which was mostly based on CCD frames in the *B*, *V*, and *R* bands. Our work is motivated by the observation that *U*-band surface brightness profiles are much less subject to the discreteness effects of individual bright red giants than those obtained at longer wavelength passbands (see King 1985). Most of the contribution to the surface brightness profile is due to the most massive nondegenerate stars in the cluster—giants, horizontal-branch stars, subgiants, and turnoff stars. This sequence represents the bright end of a rising luminosity function. While there is a relatively small variation in mass along the sequence, there is a large decrease in stellar luminosity. The relative contribution from each group to the surface brightness profile depends on the passband, since the magnitude contrast between the giant branch tip and the horizontal branch is reduced as the passband becomes bluer. As a result, *U*-band surface brightness profiles represent the contributions of larger numbers of stars and thus have significantly smaller fluctuations due to Poisson statistics than do profiles in the *B*, *V*, or *R* bands. With this motivation, a major goal of our work has been to obtain high-quality *U*-band imaging of the central regions of clusters.

In Paper I, we presented *U*-band surface brightness profiles for two clusters with well established central surface brightness cusps (NGC 6624 and NGC 7078) and one normal comparison cluster (NGC 6388). A particular emphasis of our work has been to fit *seeing-convolved* models to our profiles, in order to properly account for the effect of seeing on determined core sizes and cusp slopes. We have estimated cusp slopes by fitting

[1] Visiting Astronomer, Cerro Tololo Inter-American Observatory (CTIO), which is operated by the Association of Universities for Research in Astronomy, Inc., under contract with the National Science Foundation.

[2] Visiting Astronomer, Canada-France-Hawaii Telescope (CFHT), which is operated by the National Research Council of Canada, the Centre National de la Recherche Scientifique of France, and the University of Hawaii.

[3] Stetson (1991) has advocated the alternative description "central-cusp cluster," which is not bound to a particular theoretical interpretation.

seeing-convolved power laws, thus providing an important datum for theoretical modeling of collapsed-core clusters. No detailed treatment of seeing effects was done in the study of Djorgovski & King (1986). Instead, they fitted a pure power law over the region from 2″–3″ to 20″–30″; data from near the seeing-disk region were thus excluded. In their recent estimation of core structure parameters for all of the known Galactic globular clusters, Trager, Djorgovski, & King (1993) have made no explicit corrections for seeing effects in fitting King models.

In this paper, we present *U*-band profiles for the 15 least reddened of the 21 globular clusters (including NGC 6624 and NGC 7078) identified as having collapsed cores in the survey of Djorgovski & King (1986). We have fitted these profiles with seeing-convolved power laws, both with and without cores, in order to quantify the central structure of the clusters. Some preliminary results from this analysis have previously been reported in Lugger et al. (1991). We describe our data set in § 2 and review our data analysis procedures in § 3. We present the results of our analysis in § 4 and present our conclusions and a comparison with other recent studies of globular cluster core structure in § 5.

2. THE DATA SET

In our survey of globular cluster core structure, we have obtained CCD frames for 72 clusters, with *BVR* frames for all clusters and *U* frames for all but the most reddened clusters [i.e., $E(B-V) \lesssim 1$]. This database includes 20 of the 21 clusters that are classified as definite PCC by Djorgovski & King (1986). The *U* frames that we obtained for the 15 least reddened of these clusters [$E(B-V) \leq 0.9$] form the data set for this study; we will analyze our *B* frames for the other five clusters separately. These 15 clusters are listed in Table 1, together with some properties from the compilation by Webbink (1985). We note the recent compilation of cluster properties by Djorgovski (1993). We have chosen to list Webbink's values, since the fits presented here are based on Webbink's distance estimates. In any case, there are no major differences between the properties for these clusters in the two compilations. For example, the rms relative difference in solar distance is only about 6%.

TABLE 1

CLUSTER SAMPLE

Cluster	R_0 (kpc)[a]	R_{GC} (kpc)[b]	$E(B-V)$	[Fe/H]	M_V	r_t (pc)[c]
NGC 5946	9.2	5.1	0.56	−1.34	−7.12	26.6
NGC 6284	10.3	2.2	0.28	−1.34	−7.10	29.8
NGC 6293	7.7	1.6	0.35	−1.85	−7.39	32.9
NGC 6325	6.2	2.8	0.86	−2.02	−6.14	17.9
NGC 6342	11.6	3.4	0.46	−0.75	−6.96	29.5
NGC 6355	7.1	1.8	0.73	−1.34	−6.92	15.7
NGC 6397	2.2	6.9	0.18	−2.02	−6.55	24.7
NGC 6453	10.7	2.1	0.61	−1.51	−7.32	15.6
NGC 6522	6.6	2.3	0.49	−1.56	−7.30	19.1
NGC 6558	8.8	0.9	0.43	−1.51	−6.28	16.2
NGC 6624	8.0	1.5	0.29	−0.84	−7.46	26.8
NGC 6681	9.3	2.1	0.05	−0.92	−7.05	29.6
NGC 6752	4.1	5.9	0.05	−1.64	−7.72	36.5
NGC 7078	9.7	10.4	0.10	−2.06	−9.24	59.1
NGC 7099	7.2	7.2	0.06	−2.19	−7.17	33.4
Mean	7.9	3.7	0.37	−1.53	−7.18	27.6
Standard deviation	2.4	2.6	0.25	0.44	0.69	10.8

[a] Solar distance.
[b] Galactocentric distance.
[c] Tidal radius.

We observed the 14 southern clusters in our sample during runs in 1985 May and 1986 August on the CTIO 4 m telescope, using the Prime Focus CCD system with an RCA chip. We observed the northern cluster NGC 7078 in 1986 July using the Canada-France-Hawaii 3.6 m Telescope (CFHT) with the FOCAM imager and a double-density RCA chip. The CTIO PFCCD-RCA system has a 320 × 512 CCD format with a pixel size of 0.″59, providing a field of 3.′2 × 5.′0. The CFHT FOCAM-RCA2 system has a 640 × 1024 format with a pixel size of 0.″21, providing a 2.′2 × 3.′6 field. All of the clusters were observed through standard *UBVR* filters. The *U* filter used for most of the observations was an interference type kindly provided by M. Aaronson. Clusters were generally centered in the CCD frame, except where offsets were used to exclude extremely bright stars from the frame to avoid saturation effects. Significant offsets were used for NGC 6342, NGC 6522, NGC 6624, and NGC 6681. Paper I provides additional details of our observing technique. Table 2 lists the telescope, observation date, exposure time, and the point-spread function (PSF) FWHM for each of the frames.

3. ANALYSIS PROCEDURE

3.1. *Centering*

As discussed in Paper I, we determined cluster centers using the two-dimensional autocorrelation method of Djorgovski & King (1984) (see also review by Djorgovski 1987). This method is similar to that of Hertz & Grindlay (1985), which uses one-dimensional autocorrelations for determining the two center coordinates separately. Our tests indicate that total-light–autocorrelation centering is the best method to use for clusters observed with our median CTIO resolution of 1.″4 FWHM. Other recently used methods, such as equibarycentric centering (Aurière 1982) and residual-light–autocorrelation centering (Lauer et al. 1991), require that the image be decomposed into individual stars and an unresolved component. These methods are superior to total-light–autocorrelation centering for subarcsecond resolution ground-based and *HST* imaging where at least several tens of stars can be resolved within about 2″ of the cluster center (see Grabhorn et al. 1993). However, the images of individual bright stars are blended within the central 1″–2″ of the images used in the present study; fainter stars are completely unresolved in this region.

TABLE 2

CCD FRAMES

Cluster	Telescope	Date	Exposure (s)	FWHM
NGC 5946	CTIO 4 m	1985 May 13	1200	1.″3
NGC 6284	CTIO 4 m	1985 May 13	1200	1.3
NGC 6293	CTIO 4 m	1985 May 13	1200	1.3
NGC 6325	CTIO 4 m	1986 Aug 09	900	1.3
NGC 6342	CTIO 4 m	1985 May 12	1200	1.7
NGC 6355	CTIO 4 m	1986 Aug 09	360	1.4
NGC 6397	CTIO 4 m	1985 May 05	180	1.4
NGC 6453	CTIO 4 m	1986 Aug 09	150	1.5
NGC 6522	CTIO 4 m	1985 May 15	600	1.9
NGC 6558	CTIO 4 m	1985 May 15	1200	2.0
NGC 6624	CTIO 4 m	1985 May 13	1000	1.4
NGC 6681	CTIO 4 m	1985 May 15	600	1.9
NGC 6752	CTIO 4 m	1985 May 14	243	1.3
NGC 7078	CFHT 3.6 m	1986 Jul 28	600	0.8
NGC 7099	CTIO 4 m	1986 Aug 07	240	1.2

In order to test the reproducibility of the total-light–autocorrelation centers, we experimented with several different sizes for the data window used in the centering: 25, 50, and 100 pixels on a side (corresponding to 15″, 30″, and 59″, respectively, for the CTIO frames). The median shift in location of the center is 0.″8 both between the 25 and 50 pixel windows and between the 50 and 100 pixel windows. While these differences do not affect the behavior of the determined profiles at intermediate and large radii, there can be significant differences in the behavior of the profiles within about 2″ of the cluster center. Visual comparison of the centers produced by the different window size choices indicates that the 25 pixel windows produce centers which are most nearly coincident with the central surface brightness peak. This is expected, since the central surface brightness peak increasingly dominates the portion of the image within the centering window as the window size is reduced. We have used the 25 pixel window centers in determining the profiles for all clusters except NGC 6355. In this case, there is no well-determined peak in the surface brightness distribution and the center produced by the 50 pixel window lies closer to the apparent center of symmetry of the fairly large core (see § 4.).

3.2. *Profile Determination and Fitting*

Surface brightness profiles were determined using the octant method of Djorgovski & King (1984), as discussed in Paper I. A logarithmically spaced set of concentric circular annuli is constructed about the cluster center, and pixels are assigned to the octants of these annuli based on the location of the pixel centers. For most clusters, a grid of 25 annuli that spans the range 0.″6–120″ was used. For each annulus, the surface brightness value and its uncertainty are estimated as the mean and standard error of the mean, respectively, over the octants of that annulus. Our adopted radial binning tends to oversample the seeing FWHM by about a factor of 2 for the inner few annuli. To compensate for this effect, the weightings of these oversampled bins are set equal to the ratio of the bin width to the FWHM when performing model fits to the surface brightness profiles.

In Paper I, we considered seeing-convolved fits of both single-mass King models and power laws. In order to carry out the fits in a more unified way in the present study, we have adopted a single *modified* power–law model that covers both of these cases:

$$S(r) = S_0\left[1 + \left(\frac{r}{r_0}\right)^2\right]^{\alpha/2} . \quad (1)$$

Here r_0 is a radial scale related to the core radius, r_c, and α is the power-law index. If we adopt the usual definition of r_c as the point at which the surface brightness decreases to half of its central value, then

$$r_c = (2^{-2/\alpha} - 1)^{1/2} r_0 . \quad (2)$$

In order to include the case of a pure power law (i.e., $r_0 = 0$), the following functional form was actually fitted to the profiles:

$$S(r) = C_0(r_0^2 + r^2)^{\alpha/2} , \quad (3)$$

where $C_0 = S_0 r_0^{-\alpha}$.

For $\alpha = -2$, the profile described by equation (1) is known as an "analytic King model." In this case, $r_c = r_0$. While the analytic King model closely approximates the behavior of actual King models for $r \lesssim 3r_c$, the asymptotic large r behavior

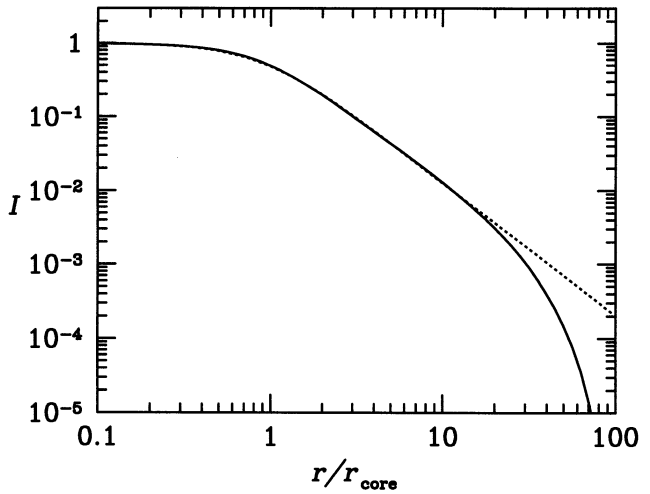

FIG. 1.—Analytic approximation to a $c = 2$ ($W_0 = 8.5$) King model. The solid curve is the exact, projected King model. The dashed curve is the analytic approximation, $S(r) = S_0[1 + (r/r_0)^2]^{-0.9}$, with $r_0 = 0.89r_c$.

of this analytic model is steeper than that for large–central concentration King models. However, for $\alpha = -1.8$ and $r_0 = 0.89r_c$, equation (1) provides an excellent approximation to a single-mass King model with central concentration parameter $c = 2$ (corresponding to central potential parameter $W_0 = 8.5$), as can be seen in Figure 1. The accuracy of the fit is better than 3% for $r \leq 14r_c$. At larger r, the King model falls increasingly below the modified power-law fit, reflecting the tidal cutoff of the former. Since the surface brightness profiles presented here do not cover the tidal cutoff region, this modified power-law approximation to a $c = 2$ King model,

$$S(r) = S_0\left[1 + \left(\frac{r}{0.89r_c}\right)^2\right]^{-0.9} , \quad (4)$$

is adequate for testing King model fits to the profiles. Thus, we did not separately perform exact King model fits. We also note that equation (1) provides a reasonable fit to a $c = 2.5$ ($W_0 = 10.75$) King model for $\alpha = -1.5$ and $r_0 = 0.80r_c$; this central concentration has been adopted as the canonical value for post–core collapse morphology by Trager et al. (1993).

We performed χ^2-minimization fits of equation (3), convolved with the seeing profile determined from each frame, to the observed cluster profiles. The convolution method, which uses a double-Gaussian form for the seeing profile, is described in Paper I. As mentioned in § 3.2, the radial oversampling of the PSF for the inner points was compensated for by weighting these points by a factor equal to the ratio of the bin width to the seeing FWHM.

The fits were performed both with and without cores. We shall refer to these as *modified* power-law fits and *pure* power-law fits, respectively. For the modified power-law fits, both r_0 and α were allowed to vary, in order to test the evidence for resolved cores. (The normalization parameter C_0 was allowed to vary in all of the fits.) In some cases, a best-fit value of $r_0 = 0$ resulted, consistent with an unresolved core. A resolved core is indicated by an apparent core radius that exceeds the radius of the seeing disk by about a factor of 3 (Lauer 1985). The profiles were fitted from the center to an outer radius r_{max}, which was cycled through the range 0.25–4 pc. This use of a range of r_{max} is motivated by the observation that the profiles typically steepen with increasing radius beyond about 0.5 pc and thus

cannot be well fitted with a single power-law slope for large values of r_{max}.

In order to place upper limits on the best-fit core radius values produced by the varying-r_0 fits, the modified power-law fits were redone with fixed r_0 stepped through increasing values until the reduced χ^2 values (i.e., χ^2 per degree of freedom) were increased by unity from the minima. For these fits, only a single value of $r_{max} = 0.5$ pc was used for all clusters except NGC 6355, for which the entire radial profile was used since the core radius is so much larger for this cluster than for the others. For clusters with upper limits on r_c exceeding 8″, additional fits were carried out with the slope fixed at -1.8, to approximate a single-mass King model. The entire radial profiles were used for these King-type fits.

For the pure power-law fits, r_0 was fixed at zero so that equation (3) represents a power-law with slope α. As in the case of the modified power-law fits, r_{max} was cycled through the range 0.25–4 pc.

4. RESULTS OF PROFILE FITS

4.1. *Fits with Cores*

Table 3 lists the results of the modified power-law fits. For each cluster, the best-fit values of r_c and α are listed, together with the value of χ^2/n_{df} for the fit. The number of degrees of freedom, n_{df}, was calculated by subtracting the number of fitting parameters from the sum of the weights, i.e., the number of independent radial bins was counted rather than the total number of bins. Also given in this table are the upper limits on core radius, $r_{c,max}$, for which $\Delta\chi^2/n_{df} = 1$, relative to the minima. The core radii and upper limits are given in both arcseconds and parsecs. The fits are shown in Figures 2*a*–2*o*, along with the pure power-law fits (see § 4.2). The fits are grouped by resolution class—unresolved cores (first nine clusters), marginally resolved cores (next three clusters), and resolved cores (final three clusters)—as described below.

The χ^2/n_{df} values listed in Table 3 represent a formal estimate of the goodness of fit. While $\chi^2/n_{df} \sim 1$ is expected for a good fit, values in the range 2–3 are found in some cases for fits that appear to be reasonable, e.g., for NGC 5946. This occurs in cases where the formal uncertainty in the surface brightness for one or more radial bins is quite small.

Nine of the clusters—NGC 5946, NGC 6284, NGC 6293, NGC 6325, NGC 6342, NGC 6558, NGC 6624, NGC 6681, and NGC 7078—have apparently unresolved cores, i.e., the upper limits on their core radii are less than 1.″9, which is 2.7 times the median seeing disk radius. As can be seen in Figure 2*a*–2*i*, the modified power-law and pure power-law fits have a very similar (or identical) small-r behavior for each of these clusters, showing that any intrinsic central flattening in the underlying profile cannot be clearly distinguished from the effects of seeing. We note that this result is somewhat dependent on the determination of the cluster center. As discussed in § 3.1, a change in the size of the centering window by a factor of 2 results in a median shift in the center position by 0.″8. Our choice of a 25 pixel centering window tends to produce centers that track the central surface brightness peak closely and thus maximizes the likelihood that an unresolved core will be detected as unresolved. By the same token, this procedure also increases the chance of a false positive detection of a resolved core as unresolved.

We note that Lauer et al. (1991) have reported the resolution of a 2.″2 core radius in M15 (= NGC 7078), based on the profile of the residual unresolved light distribution in a *Hubble Space Telescope* (*HST*) Planetary Camera image following the subtraction of the resolvable stars by a PSF-fitting procedure. However, Grabhorn et al. (1993, 1994) and Yanny (1993) have argued, on the basis of simulated prerepair *HST* imaging, that analysis of the residual light profile produced by this procedure will always indicate a resolved core, regardless of the underlying structure of the cluster. This limitation results from the difficulty in accurately subtracting bright stars given the large halo of the prerepair *HST* PSF. Grabhorn et al. (1993, 1994) and Yanny (1993) find that star counts give the most reliable measure of the cluster central structure. Yanny has estimated an upper limit of 1.″5 for the core radius of M15, based on star counts in deep *HST* Planetary Camera images, which is similar to our present estimate of $r_c \leq 1.''4$. Merritt & Tremblay (1994) have analyzed *HST* star counts for M15 from Yanny et

TABLE 3

MODIFIED POWER-LAW FITS FOR $r_{max} = 0.5$ PARSECS

Cluster	$-\frac{d\ln S}{d\ln r}$	r_c	r_c (pc)	χ^2/n_{df}	$r_{c,max}$	$r_{c,max}$ (pc)
NGC 5946	0.77 ± 0.12	0.″8 ± 0.″9	0.03 ± 0.04	3.0	1.″6	0.07
NGC 6284	0.78 ± 0.05	0	0	1.8	0.9	0.04
NGC 6293	0.72 ± 0.06	0	0	2.3	0.5	0.02
NGC 6325	0.85 ± 0.11	0	0	3.1	0.4	0.01
NGC 6342	0.89 ± 0.18	1.0 ± 1.0	0.05 ± 0.06	3.0	1.7	0.09
NGC 6355[a]	1.95 ± 0.21	15.5 ± 2.6	0.53 ± 0.09	1.0	20.3	0.70
NGC 6397	0.71 ± 0.09	3.9 ± 2.6	0.04 ± 0.03	0.9	10.5	0.11
NGC 6453	0.90 ± 0.09	1.9 ± 0.7	0.10 ± 0.04	0.6	3.3	0.17
NGC 6522	0.96 ± 0.09	2.0 ± 0.6	0.06 ± 0.02	1.6	2.7	0.09
NGC 6558	0.90 ± 0.08	0.6 ± 0.6	0.03 ± 0.02	0.4	1.9	0.08
NGC 6624	1.01 ± 0.07	1.0 ± 0.4	0.04 ± 0.02	2.1	1.6	0.06
NGC 6681	0.75 ± 0.05	0	0	1.7	0.5	0.02
NGC 6752	0.97 ± 0.15	6.7 ± 1.9	0.13 ± 0.04	1.1	8.5	0.17
NGC 7078	0.68 ± 0.02	0.8 ± 0.2	0.04 ± 0.01	0.2	1.4	0.07
NGC 7099	0.90 ± 0.07	1.9 ± 0.5	0.06 ± 0.02	0.6	3.4	0.12
Mean[b]	0.84	1.5	0.04	1.6	2.8	0.08
Standard deviation[b]	0.10	1.8	0.04	1.0	2.9	0.05

[a] $r_{max} = 2.0$ pc.
[b] Excluding NGC 6355.

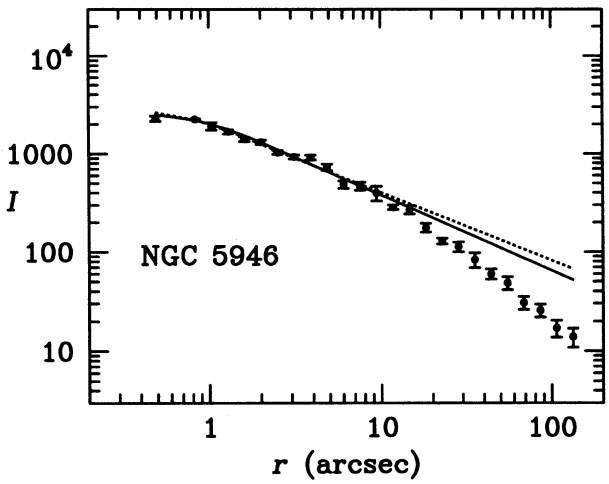

FIG. 2a

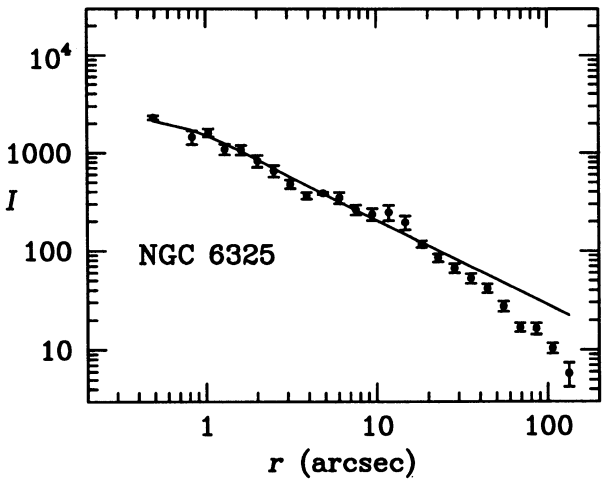

FIG. 2d

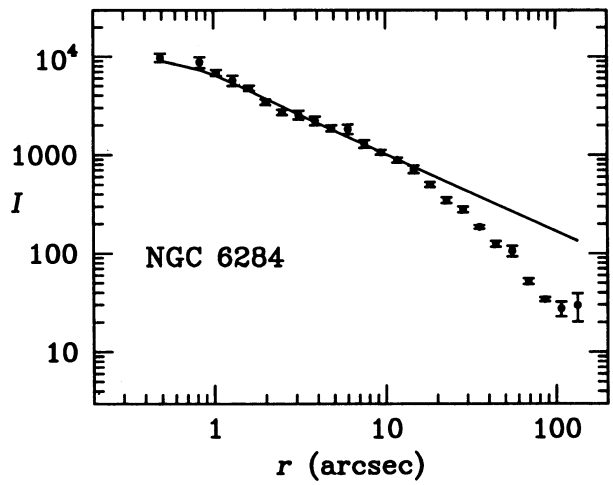

FIG. 2b

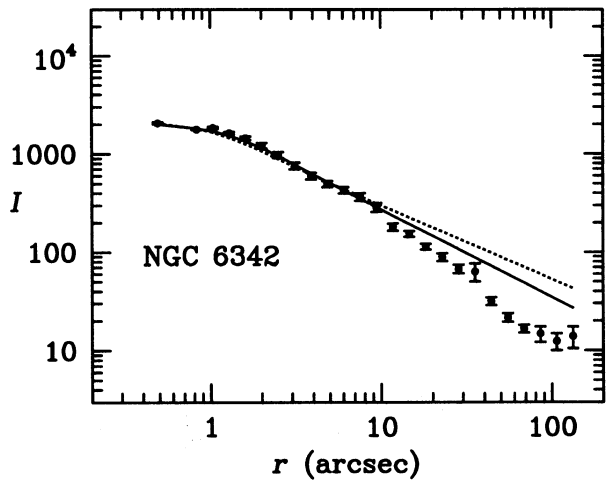

FIG. 2e

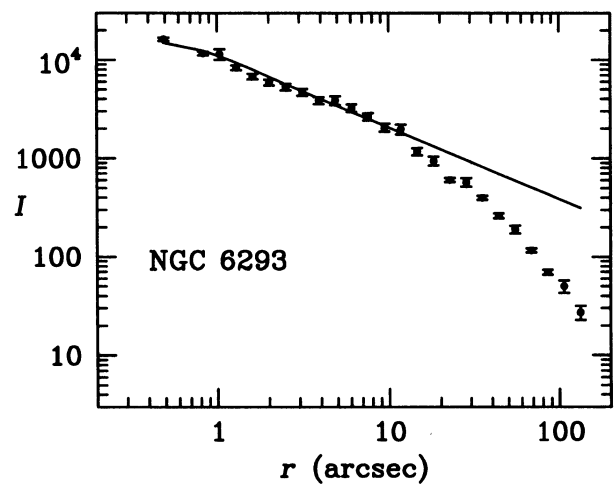

FIG. 2c

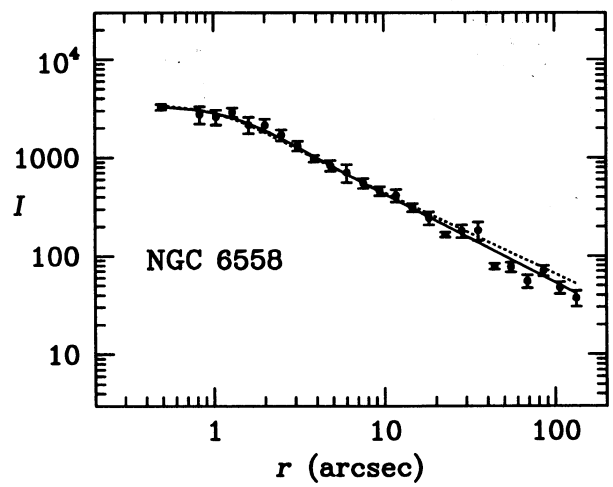

FIG. 2f

FIG. 2.—Seeing-convolved fits to surface brightness profiles. The solid curves are modified power laws; the dashed curves are pure power laws. In cases where the best-fit core radius is zero, the two fits are identical, and only one curve is seen. The clusters are grouped in columns by resolution class. (*a–i*) These nine clusters (NGC 5946, NGC 6284, NGC 6293, NGC 6325, NGC 6342, NGC 6558, NGC 6624, NGC 6681, and NGC 7078) have unresolved cores. (*j–l*) These next three clusters (NGC 6453, NGC 6522, and NGC 7099) have marginally resolved cores. (*m–o*) These last three clusters (NGC 6355, NGC 6397, and NGC 6752) have resolved cores. (*p–r*) These final panels show fits of an analytic approximation to a $c = 2$ King model (see Fig. 1) to the profiles of the three clusters with resolved cores.

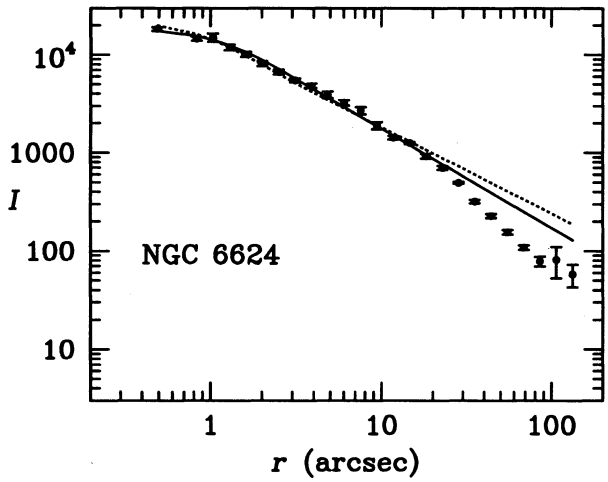

FIG. 2g

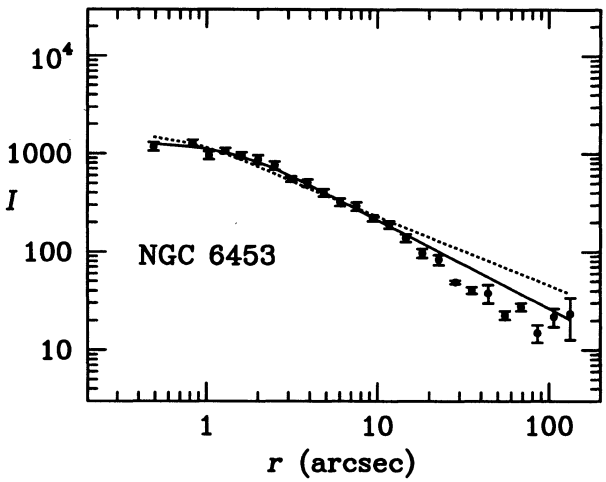

FIG. 2j

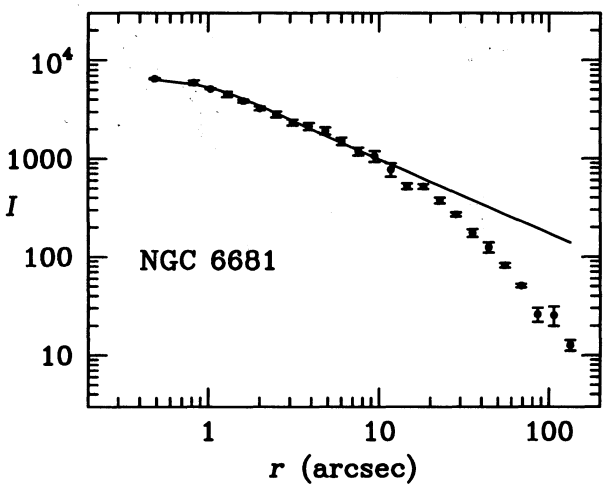

FIG. 2h

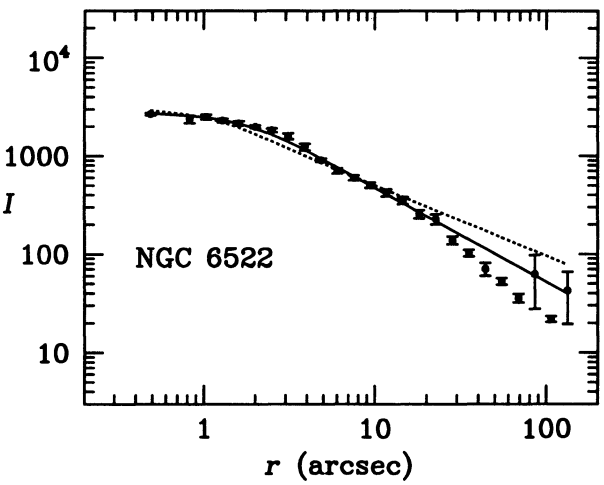

FIG. 2k

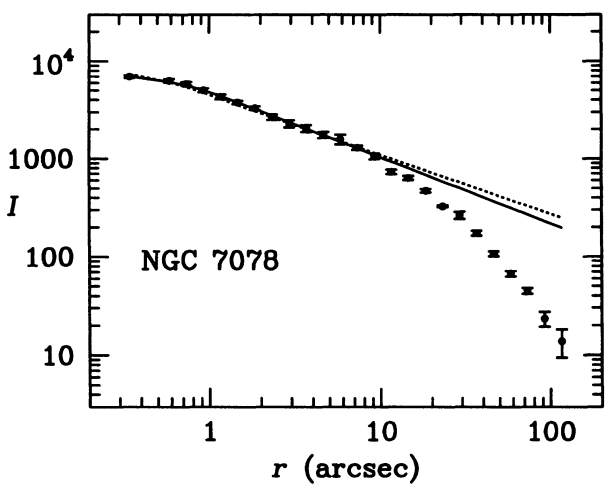

FIG. 2i

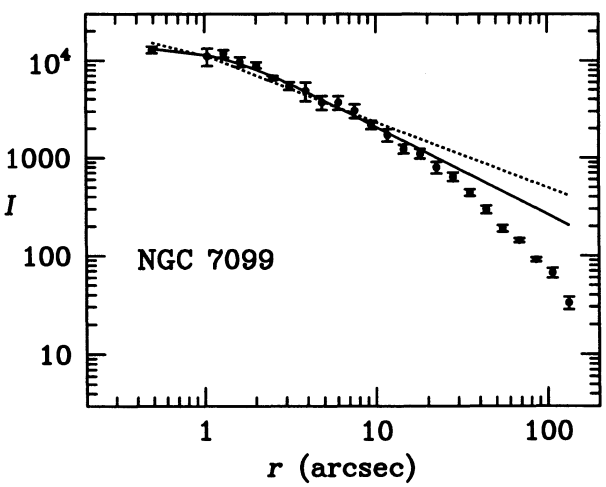

FIG. 2l

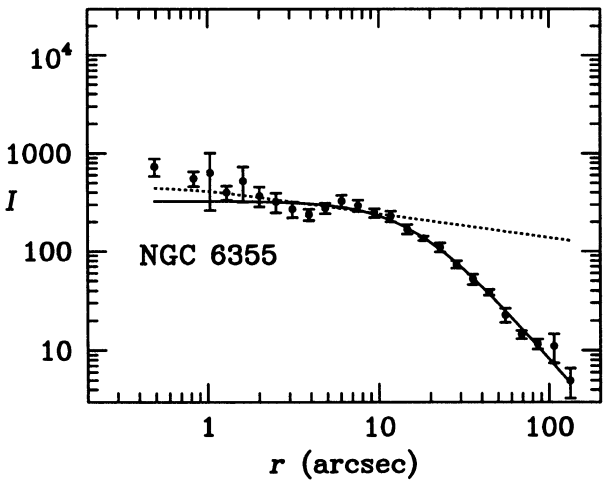

FIG. 2*m*

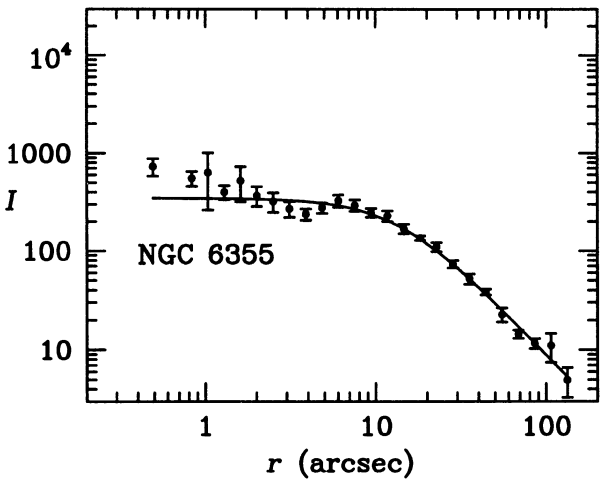

FIG. 2*p*

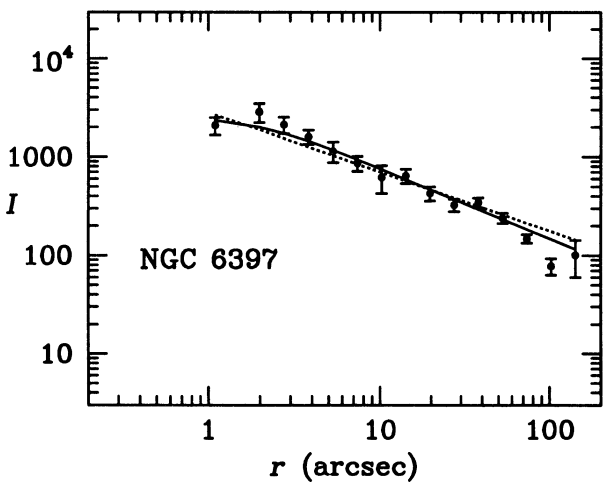

FIG. 2*n*

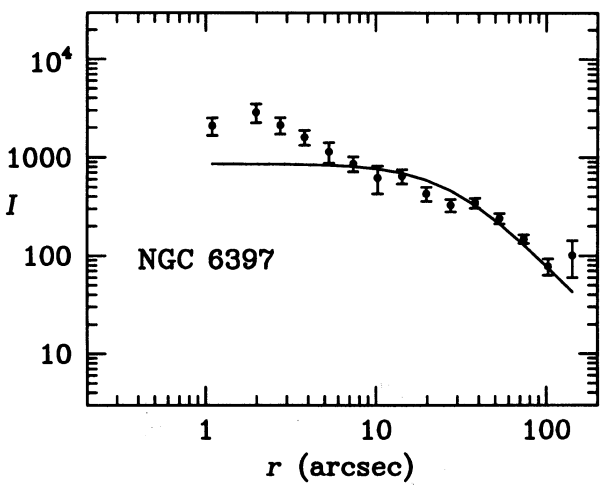

FIG. 2*q*

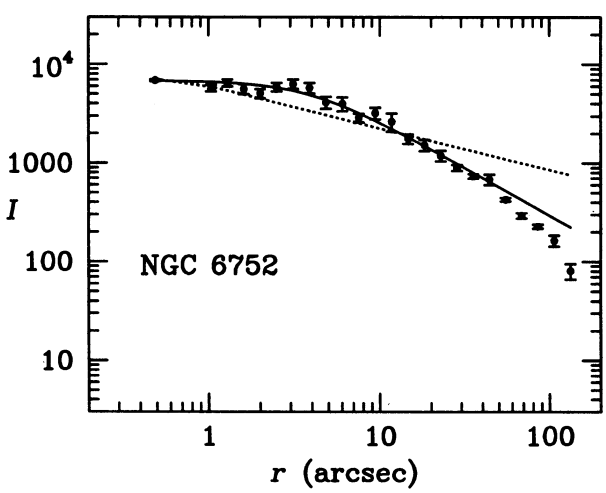

FIG. 2*o*

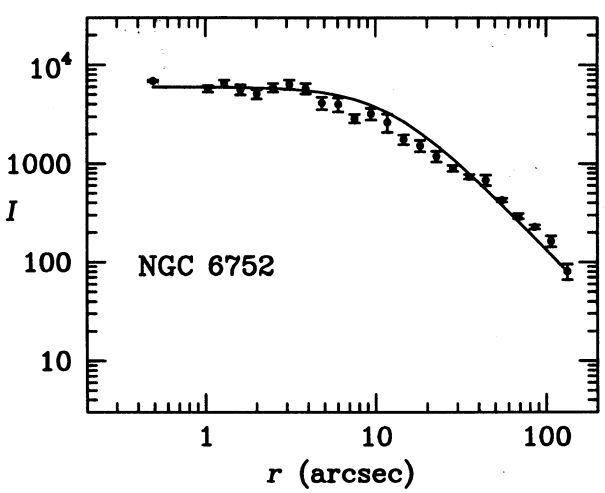

FIG. 2*r*

al. (1994), using nonparametric density estimation. Merritt & Tremblay (1994) conclude that there is no evidence for a resolved core.

Three of the clusters—NGC 6453, NGC 6522, and NGC 7099—have marginally resolved cores; the upper limits on their core radii lie in the range $2''.7 \leq r_c \leq 3''.4$. For these clusters, the best-fit values of r_c, for $r_{max} = 0.5$ pc, are all close to 2″. Within the central 5″, the pure power-law fits deviate from the modified power-law fits by a larger amount than for the nine clusters with unresolved cores (see Fig. 2*j*–2*l*).

The remaining three clusters—NGC 6355, NGC 6397, and NGC 6752—have clearly resolved cores, with upper limits exceeding 8″ (see Fig. 2*m*–2*o*). The comparison of the modified and pure power-law fits is discussed in § 4.2, below. Figure 2*p*–2*r* shows fits of the King model approximation (eq. [4]) to these clusters. This fit, in which the slope is fixed at -1.8, is quite similar to the unrestricted, modified power-law fit to NGC 6355, indicating that this cluster has the structure of a single-mass King model. There is a modest surface brightness excess at the center of an otherwise flat core.

The King model also gives a reasonable fit to the profile of NGC 6752, although the profile drops somewhat below this fit in the region 5″–30″. Comparison of Figures 2*o* and 2*r* indicates that the modified power-law fit, which produces a slope of -0.97, is somewhat better than the King model fit, out to about 1′. The determined core radii for the two fits are significantly different, $6''.7 \pm 1''.9$ for the modified power-law compared with $13''.7 \pm 0''.9$ for the King model. Aurière & Ortolani (1989) obtain a similar slope of -0.95 for the power-law region (3″–1′) and, like Djorgovski & King (1986), conclude that this cluster is in a postcollapse state. However, given that there is a reasonable King model fit, a conservative interpretation is that NGC 6752 is not required to be in a postcollapse state.

The modified power-law fit to the central 2′ of NGC 6397 is clearly better than the King model fit over this range. Nevertheless, the core of this cluster appears to be resolved. The surface brightness does not appear to increase inside of 2″, although stellar discreteness effects make this measurement difficult. Lauzeral et al. (1992) have concluded, from an analysis of high angular resolution, ground-based imaging, that NGC 6397 has a resolved core of radius 6″, corresponding to 0.07 pc. This is consistent with our best-fit value of $3''.9 \pm 2''.6$ and our upper limit of 10″.5. Lauzeral et al. (1992) interpret the detection of a resolved core surrounded by power-law structure with slope ~ -0.7 as an indication that the cluster is in an expanded-core, postcollapse state. As can be seen from Figure 2*g*, the relatively large surface brightness error bars for NGC 6397 do not strongly constrain model fits within a few arcseconds of the cluster center. This point has been emphasized by Meylan & Pryor (1993). The size of the error bars results primarily from the proximity of NGC 6397 ($R_0 = 2.2$ kpc), which results in a much higher physical resolution than for the median cluster distance of 8.0 kpc for this sample.

Drukier (1993) has compared the Lauzeral et al. (1992) surface brightness profile for NGC 6397 to profiles predicted by Fokker-Planck models that undergo core oscillations. He concludes that an expanded-core model with $r_c = 6''$ provides the best fit but that an unresolved core cannot be ruled out. This ambiguity is due to the large statistical uncertainties of the predicted profiles. Meylan & Pryor (1993) argue that dynamical models for this cluster should be fitted to a much wider radial range than the central 2′, given the proximity of NGC 6397. Drukier (1994) has in fact carried out such a program, using star count data for the outer region from Drukier et al. (1993).

We note that the median distances for the three resolution classes vary systematically—9.2 kpc for unresolved cores, 7.2 kpc for marginally resolved cores, and 4.1 kpc for resolved cores. Not surprisingly, the cores of nearer clusters are more easily resolved. However, the variation in intrinsic core size also plays a role. Of the three clusters with resolved cores, NGC 6355 and NGC 6752 have the two largest physical core radii in the sample. These are 0.53 pc and 0.13 pc, respectively, compared with a mean of 0.04 pc for the sample excluding NGC 6355. Proximity is clearly responsible for the resolution of the core of NGC 6397, since the physical core radius for this cluster is no larger than the sample mean, which includes mostly unresolved cores.

4.2. *Pure Power-Law Fits*

Table 4 lists the results from the pure power-law fits. The fits for the case $r_{max} = 0.5$ pc are shown as dashed lines in Figure 2*a*–2*o*. In cases where the best modified power-law fit has zero core radius, the pure power-law fit is identical, and only one curve is seen. As for the modified power-law fits, the χ^2/n_{df} values for the pure power-law fits typically exceed unity; the mean value over all of the clusters is smallest for $r_{max} = 0.5$ pc, at $\langle \chi^2/n_{df} \rangle = 2.3$. We interpret this value as primarily indicating that the octant method estimates for the surface brightness uncertainties are too small in some cases.

For the nine clusters that have apparently unresolved cores, it can be seen that these pure power-law fits are very similar to the modified power-law fits also shown in these figures. For the three clusters with marginally resolved cores (NGC 6453, NGC 6522, and NGC 7099) the pure power-law fits fall somewhat below the observed profiles in the range 1″–5″, although the differences are not large. For NGC 6355, which has the largest resolved core in our sample ($r_c = 0.5$ pc), the pure power-law fit to the central 0.5 pc is rather flat, as expected (slope $= -0.24$). For NGC 6397, the power-law fit out to 0.5 pc is fairly similar to the modified power-law fit, reflecting the fact that the best-fit core radius is only 0.04 pc. The best-fit power-law slopes of -0.60 and -0.66 for the fits to 0.5 pc and 1.0 pc, respectively (corresponding to 47″ and 94″), are similar to the value of -0.71 obtained by Lauzeral et al. (1992) for fits out to 70″. For NGC 6752, the best power-law fit out to 0.5 pc (slope $= -0.42$) represents a rough mean between the flat core and the steeper halo. As such, the pure power-law model does not provide a good global fit to the profile of NGC 6752.

The pure power-law slopes listed in Table 4 have a rather narrow dispersion about the mean for each value of r_{max}. The dispersion becomes particularly tight when NGC 6355 and NGC 6752 (the clusters with the largest resolved cores) are excluded. The mean slopes steepen with increasing r_{max}, as do the mean values of χ^2/n_{df}. For $r_{max} = 0.25$ pc and 0.5 pc, the mean slopes excluding NGC 6355 and NGC 6752 are -0.7 ± 0.1, and the χ^2/n_{df} values indicate that the fits are generally acceptable. For $r_{max} \geq 1$ pc, the χ^2/n_{df} values quickly increase beyond the range for acceptable fits, indicating that a single-slope power law is no longer sufficient to describe the behavior of the profile in most cases. For these larger values of r_{max}, the power-law slopes represent means over the radial range of the fits. Since r_{max} is a physical rather than angular radius, our comparison of cluster structure is largely independent of distance. Thus, the small dispersion in the power-law slopes and the similar physical sizes of the power-law regions

TABLE 4

PURE POWER-LAW FITS

	r_{max}									
	0.25 pc		0.5 pc		1.0 pc		2.0 pc		4.0 pc	
CLUSTER	$-\frac{d\ln S}{d\ln r}$	χ^2/n_{df}	$-\frac{d\ln S}{d\ln r}$	χ^2/n_{df}	$-\frac{d\ln S}{d\ln r}$	χ^2/n_{df}	$-\frac{d\ln S}{d\ln r}$	χ^2/n_{df}	$-\frac{d\ln S}{d\ln r}$	χ^2/n_{df}
NGC 5946	0.64	3.2	0.69	2.8	0.75	4.0	0.82	7.0	0.87	9.6
NGC 6284	0.81	2.1	0.78	1.4	0.84	2.2	0.98	9.8	1.08	20.4
NGC 6293	0.74	3.4	0.72	1.9	0.87	8.1	0.92	9.7	1.04	27.9
NGC 6325	0.87	3.1	0.85	2.6	0.89	2.3	0.93	3.0	1.00	6.5
NGC 6342	0.71	7.5	0.75	3.0	0.84	5.4	0.89	5.8	0.98	15.5
NGC 6355	0.36	2.0	0.24	1.2	0.58	4.4	0.77	11.2	0.90	17.8
NGC 6397	0.58	1.2	0.60	1.2	0.66	1.7	0.70	2.5	0.70	2.5
NGC 6453	0.58	3.7	0.70	1.9	0.78	3.2	0.94	10.4	0.95	9.1
NGC 6522	0.69	12.1	0.72	5.8	0.78	8.9	0.89	18.3	0.95	23.3
NGC 6558	0.81	1.0	0.83	0.4	0.91	1.7	0.95	2.6	0.94	2.5
NGC 6624	0.78	0.3	0.88	3.9	0.91	4.9	1.02	25.1	1.08	40.3
NGC 6681	0.76	3.1	0.75	1.1	0.82	2.8	0.89	7.8	1.04	34.1
NGC 6752	0.30	2.3	0.42	4.9	0.53	7.9	0.66	18.6	0.68	21.7
NGC 7078	0.58	1.2	0.60	1.2	0.71	8.2	0.79	20.6	0.90	65.0
NGC 7099	0.57	1.6	0.67	2.2	0.79	3.9	0.94	10.9	1.02	16.4
Mean	0.65	3.2	0.68	2.4	0.78	4.6	0.87	10.9	0.94	20.8
Standard deviation	0.11	3.2	0.15	1.6	0.12	2.4	0.10	6.5	0.09	16.1
Mean[a]	0.70	3.3	0.73	2.3	0.81	4.4	0.90	10.3	0.97	21.0
Standard deviation[a]	0.10	2.9	0.08	1.3	0.07	2.4	0.08	6.6	0.10	16.6

[a] Excluding NGC 6355 and NGC 6752.

suggest that central-cusp clusters have a common physical structure.

The slope and size of the central-cusp region depend on characteristics of the stellar population, e.g., the number and mass distribution of heavy nonluminous remnants. Thus, it appears that these characteristics do not vary greatly within the sample of central-cusp clusters. Kinematic determinations of central mass-to-light ratios would provide a robust test of this surmise, since this ratio depends sensitively on the nonluminous remnant population.

5. DISCUSSION

5.1. *Comparison with Other Observational Studies*

In their large-scale survey of cluster core structure, Djorgovski & King (1986) classified a cluster as having a collapsed core if the profile could not be fitted by a single-mass King model of moderate to high central concentration. Of our present sample of 15 candidate collapsed-core clusters identified by Djorgovski & King (1986), we find that there are reasonable single-mass King model fits to two of these clusters. There appears to be no evidence to support a collapsed-core interpretation of our *U*-band profile of NGC 6355, which has significantly smaller statistical uncertainty than the *B*-band profile analyzed by Djorgovski & King (1986). In the case of NGC 6752, the modified power-law fit to our profile is somewhat better than the King model fit, although the difference is not large. Thus, the evidence supporting the collapsed-core interpretation of this profile is not strong.

Djorgovski & King (1986) did not specifically address the question of whether any of the cores that they identified as collapsed might nevertheless be resolved. These two states are not necessarily mutually exclusive, especially in the case of the nearer clusters in the sample. For example, NGC 6397 appears to have a collapsed but resolved core. We find nine of the 15 clusters in our sample to have unresolved cores, three to have marginally resolved cores, and three to have resolved cores. The three marginally resolved cores, which also appear to be collapsed, have upper limits of about 3″. Thus, our finding that these cores are marginally resolved is not in conflict with the results of Djorgovski & King (1986), since they excluded data from the inner 2″–3″ radius about the cluster center in order to eliminate the effect of seeing on their power-law fits. As a result, their analysis is not sensitive to a core size of $r_c \lesssim 3''$. Examination of Figure 2 in Djorgovski & King (1986) indicates that their profiles for NGC 6355, NGC 6397, and NGC 6752 are consistent with our interpretation that the cores of these clusters are resolved. Their *B*-band profile for NGC 6355 has large error bars within a radius of 6″ that can be fitted with a flat-core model. Their *B*-band profile for NGC 6397, in contrast, has very small error bars and is quite smooth within a radius of about 10″. The seeing profile for their image of this nearby cluster is evidently rather broad. The central region of this profile is well fitted by a flat-core model. Finally, their *U*-band profile for NGC 6752 is quite flat inside of a sharp shoulder at about 4″.

As discussed in § 4.1, two of the clusters in our study, M15 and NGC 6397, have been extensively analyzed in other recent studies of globular cluster structure. We find that the core of M15 has not been resolved, with an upper limit of 1″.4, in accord with Yanny (1993) and Merritt & Tremblay (1994). Analysis of simulated prerepair *HST* Planetary Camera imaging by both our group (Grabhorn et al. 1993, 1994) and Yanny (1993) indicates that the resolution of a 2″.2 core radius by Lauer et al. (1991) is a necessary result of the analysis method they used, even if the core is considerably smaller. The greatly improved PSF that is provided by the Wide Field/Planetary Camera 2 (WFPC 2) and the Faint Object Camera

with COSPAR should help to resolve this discrepancy. However, even "perfect" resolution will produce only upper limits for very small unresolved cores ($r_c \ll 1''$), owing to the inherent graininess of the stellar distribution. We are using simulated WFPC 2 imaging to investigate the limits that can be placed on core sizes.

Our results for NGC 6397 are in good agreement with the studies of Lauzeral et al. (1992) and Drukier (1993). There is common agreement that the core of this cluster has most likely been resolved, with $r_c \sim 4''$–$6''$, although Drukier notes that the possibility of an unresolved core cannot be rejected.

The proximity of NGC 6397 makes it an excellent candidate for structure determination using star counts from *HST* imaging. We have investigated such an analysis, using the *R*-band photometry from *HST* Planetary Camera imaging reported by Cool et al. (1995). These counts appear to be complete to $R \approx 19$, which corresponds to $M_R \approx 7$. The region covered by the Planetary Camera frame containing the cluster center extends to a radius of about 15″ from the center, which is an order of magnitude smaller than the region considered in the present study. Thus, *HST* data are best used in combination with ground-based data to provide a more global view of cluster structure. In any case, the results of our analysis of these *HST* data are consistent with those obtained from ground-based imaging by the present study and by Lauzeral et al. (1992). In particular, pure power-law fits give a best-fit slope of about -0.6, which is in close agreement with the values in Table 4 for fits to the innermost part of the profile. The modified power-law fits allow a wide range of power-law slope, with a suitably adjusted core radius, owing to the narrow radial range of the *HST* data. For power-law slopes in the range -0.6 to -1.0, the corresponding range of best-fit core radius values is 2″–6″. These results will be reported in detail in a separate paper. NGC 6752, which is a factor of 2 closer than the median distance for clusters in this sample, is also a good candidate for structure studies using high-resolution *HST* imaging.

Trager et al. (1993) have estimated structural parameters for all of the known Galactic globular clusters, based on King model fitting of surface brightness profiles. For most clusters with apparent postcollapse morphology, including the 15 clusters in our sample, they set the core radius equal to the apparent half-width at half-maximum (HWHM) of the profile, without correcting for seeing. The HWHM was determined from a polynomial fit to the central profile. For the 15 clusters in our sample, Trager et al. (1993) find a mean core radius of $\langle r_c \rangle = 3''.6 \pm 2''.0$ (standard deviation). If NGC 6752, for which they estimate $r_c = 10''.5$, is excluded, the dispersion tightens and $\langle r_c \rangle = 3''.2 \pm 0''.9$. Thus, it appears that their method of estimating core radius gives a standard value of about 3″ for clusters with apparent postcollapse morphology. By comparison, the mean core radius from our modified power-law fits (excluding NGC 6355) is $\langle r_c \rangle = 1''.5 \pm 1''.8$, which is a factor of 2 smaller. The mean of our estimated upper limits on core radius, $\langle r_{c,\max} \rangle = 2''.8 \pm 2''.9$, is closer to their mean. The neglect of seeing corrections by Trager et al. (1993) is at least partially responsible for their larger core radius estimates. Since their typical seeing disk FWHM was at least 2″ (S. Trager & S. Djorgovski, 1994 private communication), their minimum resolvable core radius is 3″, using the criterion that the apparent HWHM of the profile must exceed the seeing disk radius by a factor of 3 in order for the core to be resolved (Lauer 1985).

5.2. *Comparison with Theory*

Grabhorn et al. (1992) and Grabhorn (1993) have shown that the surface brightness profiles of two of the central-cusp clusters in the present study, NGC 6624 and M15, can be fitted with detailed Fokker-Planck models for clusters evolving through core collapse. The postcollapse models are also consistent with an increase of the velocity dispersion toward the center of M15 (Peterson, Seitzer, & Cudworth 1989; Gebhardt et al. 1994; Dubath & Meylan 1994; Dull et al. 1994) and the negative period derivatives of two millisecond pulsars (PSR 2127+11A and D) that are both located 1″ from the center of this cluster (Wolszczan et al. 1989; Anderson 1993). The deep gravitational potential well that accounts for these observations is due to a central concentration of nonluminous remnants with masses in the range 1.2–1.4 $M_\odot$. It seems likely that these predicted remnants represent the same neutron star population that is responsible for the production of the nine millisecond pulsars and the single low-mass X-ray binary observed in M15. Phinney (1993) has considered a wide range of Fokker-Planck model fits to M15, varying such properties as the luminous and nonluminous mass functions, the treatment of stellar evolution, and the neutron star retention fraction. He obtains similar results to those of Grabhorn et al. (1992). In particular, these studies predict the presence of a few tens of thousands of degenerate remnants with masses exceeding about 1 $M_\odot$, of which a few thousand are likely to be neutron stars.

With the exception of NGC 6355 and NGC 6752, the clusters in our sample can all be described as having a core radius $r_c \lesssim 0.1$ pc, surrounded by a power-law profile with slope $\alpha \approx -0.8$. NGC 6752 can be described by a similar model, with a somewhat larger core (0.17 pc). This common physical structure suggests that the same postcollapse model that has been fitted to M15 may generally apply to this group. In particular, the power-law slope of the central surface brightness profile and the extent of the power-law region depend on the upper mass limit for the nonluminous remnants and the fraction of the cluster mass in the nonluminous remnant population, respectively (Murphy & Cohn 1988). Thus, it seems likely that these quantities have similar values for the 14 clusters, although M15 may represent an extreme case owing to its considerably higher total mass (inferred from total absolute magnitude) than that of the other clusters in this study. Kinematic measurements, which are sensitive to the presence of dark matter, should provide a strong test of this conjecture. Such kinematic measurements include studies of both stellar velocity distributions and millisecond pulsar accelerations. As noted by Grabhorn et al. (1992), the combination of photometric and kinematic data greatly constrains the possible range of model fits relative to the use of photometric data alone.

Postcollapse clusters are predicted to undergo large-amplitude oscillations in core size due to the gravothermal instability of collisional stellar systems. As discussed by Cohn et al. (1991), the core hovers near its maximally expanded size for most of each oscillation cycle. For the model fits to M15 presented by Grabhorn et al. (1992), a core radius as large as the 2″.2 value obtained by Lauer et al. (1991) can be accommodated. This corresponds to a physical size of 0.10 pc. Fourteen of the 15 clusters in our sample have core radius upper limits of 0.17 pc or smaller; the median upper limit is 0.08 pc. Thus, with the exception of NGC 6355, these clusters have core sizes consistent with the expectations for a postcollapse bounce.

5.3. *Future Prospects*

The choice of surface brightness profiles over star counts, for determining cluster central structure, was dictated in this study by the median 1".4 FWHM resolution. As the angular resolution of cluster imaging from both the ground and space continues to be improved, star count profiles should supplant surface brightness profiles as the best means of determining cluster structure. This is likely to occur with the refurbished *HST*. As demonstrated by Grabhorn et al. (1993), *prerepair HST* imaging does not greatly exceed the power of ground-based imaging for resolving cluster cores. With the enormous improvement in the PSF behavior provided by the repair, the power of *HST* imaging for resolving cluster cores via image decomposition techniques should be significantly increased.

The present study has focused on the portion of a cluster profile that fits within a single CCD frame of size 3′ × 5′; the determined profiles extend to 2′ from the cluster center. Meylan & Pryor (1993) have emphasized the importance of fitting dynamical models to as wide a radial range as possible of both structural and kinematic data, in order to reliably determine the dynamical state of a cluster. Thus, central surface brightness profiles of the type produced in the present study are best combined with other data sets (usually star counts) that cover the outer regions of clusters. We have taken this approach in our study of M15 and NGC 6624 (Grabhorn et al. 1992). Programs to study the structure of entire clusters will be greatly facilitated by the continuing increase in CCD format sizes and the development of mosaic imagers.

We are grateful to Charles Bailyn for many useful conversations and much encouragement. We also thank George Djorgovski and Ivan King for their helpful insights. This work was supported by NSF grants AST 88-20916 and AST 91-19965 to Indiana University and by NASA grant NAGW-3280 to Harvard University.

REFERENCES

Anderson, S. B. 1993, Ph.D. thesis, California Inst. of Technology
Aurière, M. 1982, A&A, 109, 301
Aurière, M., & Ortolani, S. 1989, A&A, 221, 20
Cohn, H. 1980, ApJ, 242, 765
Cohn, H. N., Lugger, P. M., Grabhorn, R. P., Breeden, J. L., Packard, N. H., Murphy, B. W., & Hut, P. 1991, in The Formation and Evolution of Star Clusters, ed. K. Janes (ASP Conf. Ser., 13), 381
Cool, A. M., Grindlay, J. E., Cohn, H. N., Lugger, P. M., & Slavin, S. D. 1995, ApJ, in press
Djorgovski, S. 1987, in IAU Symp. 126, Globular Cluster Systems in Galaxies, ed. J. E. Grindlay & A. G. D. Philip (Dordrecht: Kluwer), 333
———. 1993, in Structure and Dynamics of Globular Clusters, ed. S. G. Djorgovski & G. Meylan (ASP Conf. Ser., 50), 373
Djorgovski, S., & King, I. R. 1984, ApJ, 277, L49
———. 1986, ApJ, 305, L61
Drukier, G. A. 1993, MNRAS, 265, 773
———. 1994, preprint
Drukier, G. A., Fahlman, G. G., Richer, H. B., Searle, L., & Thompson, I. 1993, AJ, 106, 2335
Dubath, P., & Meylan, G. 1994, A&A, in press
Dull, J. D., Cohn, H. N., Lugger, P. M., Murphy, B. W., Seitzer, P. O., Callanan, P. J., Rutten, R. G. M., & Charles, P. A. 1994, in preparation
Gebhardt, K., Pryor, C., Williams, T. B., & Hesser, J. E. 1994, AJ, 107, 2067
Grabhorn, R. P. 1993, Ph.D. thesis, Indiana Univ.
Grabhorn, R. P., Cohn, H. N., Lugger, P. M., & Murphy, B. W. 1992, ApJ, 392, 86
Grabhorn, R. P., Dull, J. D., Irwin, J. A., Cohn, H. N., & Lugger, P. M. 1994, in preparation
Grabhorn, R. P., Irwin, J. A., Cohn, H. N., & Lugger, P. M. 1993, in Structure and Dynamics of Globular Clusters, ed. S. G. Djorgovski & G. Meylan (ASP Conf. Ser., 50), 131
Hertz, P., & Grindlay, J. E. 1985, ApJ, 298, 95
King, I. R. 1985, in IAU Symp. 113, Dynamics of Star Clusters, ed. J. Goodman & P. Hut (Dordrecht: Reidel), 1
Lauer, T. R. 1985, ApJ, 292, 104
Lauer, T. R., et al. 1991, ApJ, 369, L45
Lauzeral, C., Ortolani, S., Aurière, M., & Melnick, J. 1992, A&A, 262, 63
Lugger, P. M., Cohn, H., Grindlay, J. E., Bailyn, C. D., & Hertz, P. 1987, ApJ, 320, 482 (Paper I)
———. 1991, in The Formation and Evolution of Star Clusters, ed. K. Janes, (ASP Conf. Ser., 13), 414
Merritt, D., & Tremblay, B. 1994, AJ, 108, 514
Meylan, G., & Pryor, C. 1993, in Structure and Dynamics of Globular Clusters, ed. S. G. Djorgovski & G. Meylan (ASP Conf. Ser., 50), 31
Murphy, B. W., & Cohn, H. 1988, MNRAS, 232, 835
Newell, B., & O'Neil, E. J. 1978, ApJS, 37, 27
Peterson, R. C., Seitzer, P., & Cudworth, K. M. 1989, ApJ, 347, 251
Phinney, E. S. 1993, in Structure and Dynamics of Globular Clusters, ed. S. G. Djorgovski & G. Meylan (ASP Conf. Ser., 50), 141
Stetson, P. B. 1991, in Precision Photometry, Astrophysics of the Galaxy, ed. A. G. D. Philip, A. R. Upgren, & K. A. Janes (Schenectady: Davis), 69
Trager, S. C., Djorgovski, S., & King, I. R. 1993, in Structure and Dynamics of Globular Clusters, ed. S. G. Djorgovski & G. Meylan (ASP Conf. Ser., 50), 347
Webbink, R. F. 1985, in IAU Symp. 113, Dynamics of Star Clusters, ed. J. Goodman & P. Hut (Dordrecht: Reidel), 541
Wolszczan, A., Kulkarni, S. R., Middleditch, J., Backer, D. C., Fruchter, A. S., & Dewey, R. J. 1989, Nature, 337, 531
Yanny, B. 1993, PASP, 105, 969
Yanny, B., Guhathakurta, P., Bahcall, J. N., & Schneider, D. P. 1994, AJ, 107, 1745